

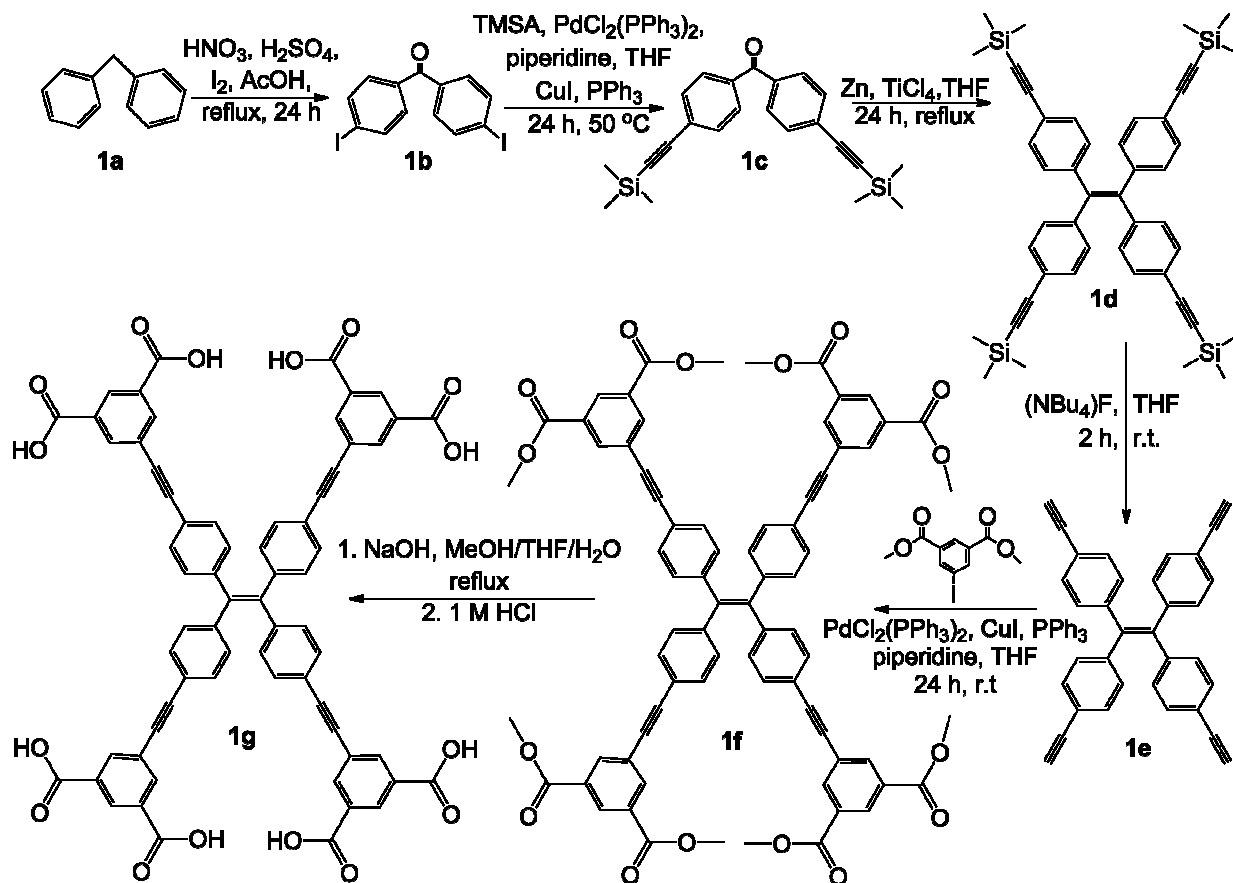
Supporting Information

Conformational Locking by Design: Relating Strain Energy with Luminescence and Stability in Rigid Metal-Organic Frameworks

Natalia B. Shustova, Anthony F. Cozzolino, Mircea Dincă*
*Department of Chemistry, Massachusetts Institute of Technology
Cambridge, Massachusetts, 02139, USA*

Table of Contents:	page number
1. Scheme S1. Synthesis of H ₈ TDPEPE	S3
2. Materials	S3
3. Synthesis of 4,4'-diiodobenzophenone	S4
4. Synthesis of 4,4'-bis(trimethylsilylethynyl)benzophenone	S4
5. Synthesis of tetrakis(4-ethynylphenyl)ethylene	S4
6. Synthesis of tetrakis(4-(meta-dimethylphthalylethynyl)phenyl)ethylene	S6
7. Synthesis of H ₈ TDPEPE	S6
8. Synthesis of 1	S6
9. Computational details	S6
10. X-ray crystal structure determination	S7
11. UV-vis and fluorescence spectroscopy	S7
12. Other physical measurements	S7
13. Figure S1. DFT-calculated potential energy surface for phenyl ring flipping for 5-((4-vinylphenyl)ethynyl)isophthalic acid	S9
14. Figure S2. The shortest chromophore-chromophore contacts in 1	S10
15. Table S1. X-ray structure refinement data for 1	S11
16. Figure S3. Normalized absorption and emission spectra for 1 and H ₈ TDPEPE	S12
17. Figure S4. PXRD patterns of 1 after heating and using a supercritical CO ₂ technique	S13
18. Figure S5. H ₈ TDPEPE and overlay of H ₈ TDPEPE and H ₈ TDPEPE\llcorner 1	S14
19. Figure S6. Simulated and experimental PXRD patterns of 1	S15

20. Figure S7. ^1H NMR spectrum of H_8TDPEPE in $\text{DMSO-}d^6$ (500 MHz)	S16
21. Figure S8. ^{13}C NMR spectrum of H_8TDPEPE in $\text{DMSO-}d^6$ (500 MHz)	S17
22. Figure S9. H_3BTE and overlay of H_3BTE and $\text{H}_3\text{BTE}\subset\text{MOF-180}$	S18
23. Figure S10. H_8TDM and overlay of H_8TDM and $\text{H}_8\text{TDM}\subset\text{PCN-26}$	S19
24. Figure S11. H_8MTBD and overlay of H_8MTBD and $\text{H}_8\text{MTBD}\subset\text{NOTT-140}$	S20
25. Figure S12. H_3BBC and overlay of H_3BBC and $\text{H}_3\text{BBC}\subset\text{MOF-200}$	S21
26. Figure S13. $\text{H}_6\text{TCAEPEB}$ and overlay of $\text{H}_6\text{TCAEPEB}$ and $\text{H}_6\text{TCAEPEB}\subset\text{NU-100}$	S22
27. Figure S14. H_8BTTCD and overlay of H_8BTTCD and $\text{H}_8\text{BTTCD}\subset\text{PCN-80}$	S23
28. Figure S15. H_8PTMT and overlay of H_8PTMT and $\text{H}_8\text{PTMT}\subset\text{Cu}_4(\text{PTMT})(\text{H}_2\text{O})_4$	S24
29. Figure S16. $\text{H}_3\text{TPT-3tz}$ and overlay of $\text{H}_3\text{TPT-3tz}$ and $\text{H}_3\text{TPT-3tz}\subset\text{Mn}_3[(\text{Mn}_4\text{Cl})_3(\text{TPT-3tz})_8]_2$	S25
30. Figure S17. H_8BTMPT and overlay of H_8BTMPT and $\text{H}_8\text{BTMPT}\subset\text{Cu}_4(\text{BTMPT})(\text{H}_2\text{O})_4$	S26
31. Figure S18. The arm ratio is exemplified with H_8TDPEPE	S27



Scheme S1. Synthesis of H₃TDPEPE.

Experimental Section.

Materials. Zn(NO₃)₂·6H₂O (98%, Strem Chemicals), diphenylmethane (99%, Sigma-Aldrich), I₂ (99.8%, Sigma-Aldrich), H₂SO₄ (98%, BDH), HNO₃ (65%, Sigma-Aldrich), glacial CH₃COOH (Mallinckrodt Chemicals), dioxane (99.8%, Sigma-Aldrich), Br₂ (≥ 99.5%, Sigma-Aldrich), PdCl₂(PPh₃)₂ (98%, Oakwood Products), PPh₃ (99%, Alfa Aesar), CuI (98%, Strem Chemicals), CuCN (99%, Strem Chemicals), Zn (dust, 98.6%, Mallinckrodt), oxalyl chloride (98%, Alfa Aesar), TiCl₄ (≥ 99%, Sigma-Aldrich), MgSO₄ (98%, VWR), *N,N'*-dimethylethylenediamine (99%, Sigma-Aldrich), CH₂Cl₂ (HPLC grade, Honeywell), CH₃OH (99.9%, VWR), *N,N*-diethylformamide (> 95%, TCI America), ethanol (ACS grade, Mallinckrodt), ethylene glycol (AR grade, Mallinckrodt), ethyl acetate (VWR), tetrahydrofuran (ACS grade, Mallinckrodt), toluene (Sigma-Aldrich, ACS), C₆D₆ (Cambridge Isotopes), CDCl₃

(Cambridge Isotopes), CD₃OD (Cambridge Isotopes), and DMSO-*d*₆ (Cambridge Isotopes) were used as received. Piperidine (99.5%, Sigma-Aldrich) was freshly distilled before use.

4,4'-diiodobenzophenone (C₁₃H₈I₂O, **1b**). Compound **1b** was prepared from diphenylmethane (**1a**) according to a reported procedure.¹

4,4'-bis(trimethylsilylethynyl)benzophenone (C₂₃H₂₆OSi₂, **1c**). In a Schlenk tube, **1b** (3.00 g, 6.91 mmol), CuI (0.263 g, 1.38 mmol), PPh₃ (0.543 g, 2.07 mmol) and PdCl₂(PPh₃)₂ (0.483 g, 0.688 mmol) were dissolved in piperidine (20 mL) and THF (60 mL). Trimethylsilylacetylene (3.86 mL, 27.3 mmol) was added and the mixture was stirred for 24 h at 50 °C. After cooling, the solvent was removed and the product was extracted in dichloromethane. The organic fraction was filtered through a Celite pad. After solvent removal, the solid product was flushed through a silica gel column (35 cm length, 2.5 cm diameter) using a 100:1 hexane/ethyl acetate eluent. Compound **1c** was isolated as a white powder (2.06 g, 5.49 mmol) with 80% yield. ¹H NMR (CDCl₃, 500 MHz): δ = 0.25 (s), 7.54 (d, *J* = 8 Hz), 7.72 (d, *J* = 8 Hz) ppm. The ¹H NMR spectra matched those reported previously for this compound.² IR (neat, cm⁻¹): 2159 (m), 1658 (s), 1602 (m), 1466 (w), 1401 (w), 1308 (m), 1290 (m), 1274 (m), 1250 (m), 1220 (w), 1174 (w), 1145 (w), 930 (w), 845 (vs), 758 (m), 650 (m).

Tetrakis(4-ethynylphenyl)ethylene (C₃₄H₂₀, **1e**). Zinc dust (1.68 g, 25.7 mmol) and **1c** (6.94 g, 18.5 mmol) were placed in 500 mL Schlenk flask, which had previously been evacuated and flushed with N₂. A volume of 350 mL of THF was added to the solid reactants under a flow of nitrogen. The reaction mixture was cooled to 0–5 °C in an ice bath and 1.39 g (7.33 mmol) of TiCl₄ was added dropwise. The mixture was warmed up during 1 h, stirred for an additional 2 h at room temperature, and heated at reflux for 24 h. After cooling to room temperature, the reaction mixture was quenched with a volume of 300 mL of a 10% K₂CO₃ solution and stirred for 3 h. The product was extracted in dichloromethane. The organic layer was dried over magnesium sulfate and the solvent was removed under reduced pressure. The crude yellow product (**1d**, 6.34 g) was dissolved in THF (200 mL), and 18.9 g (0.054 mol) of tetrabutylammonium fluoride (75% water solution) was added dropwise. After stirring for 2 hours at room temperature, water was added to the solution. The product was extracted using

chloroform, and the residual solvent was evaporated under reduced pressure. The crude product was chromatographed on a silica-gel column (35 cm length, 2.5 cm diameter) using a gradient elution starting from 10:90 to 20:80 ethyl acetate/hexane mixtures (~1 L of 10:90 ethyl acetate/hexane mixture and ~ 4 L of 20:80 ethyl acetate/hexane mixture). Compound **1d** was isolated as a yellow solid (3.65 g, 8.50 mmol) in 93% yield. ^1H NMR (CDCl_3 , 500 MHz): δ = 3.08 (s), 6.94 (d, J = 8 Hz), 7.25 (d, J = 8 Hz) ppm. The ^1H NMR data for **1d** matched those reported previously.³

Tetrakis(1-(dimethyl-3,5-carboxy-phenyl-1-ethynyl)-4-phenyl)ethylene ($\text{C}_{74}\text{H}_{52}\text{O}_{16}$, **1f**). Dimethyl 5-iodoisophthalate (11.5 g, 35.9 mmol), which was synthesized using a reported procedure⁴, PPh_3 (0.671 g, 2.56 mmol), $\text{PdCl}_2(\text{PPh}_3)_2$ (0.594 g, 0.846 mmol), and CuI (0.323 g, 1.70 mmol) were placed in a Schlenk flask that was evacuated and flushed with nitrogen. After addition of THF (150 mL) to the reaction mixture under nitrogen, a solution of **1e** (2.92 g, 6.81 mmol) in THF (130 mL) and piperidine (20 mL) was added dropwise.. The reaction mixture was stirred at room temperature for 24 h. Solvent was evaporated under reduced pressure, to yield a brown solid. This solid was dissolved in CH_2Cl_2 (500 mL) and the organic layer was washed with water, dried over anhydrous MgSO_4 , and evaporated under reduced pressure. The solid product was purified on a silica-gel column (35 cm length, 2.5 cm diameter) using ethyl acetate/hexane mixtures (slowly increasing polarity of the eluent from 10:90 ethyl acetate/hexane mixture to 50:50 ethyl acetate/hexane mixture). The final product was recrystallized from an 30:70 v:v ethyl acetate/hexane mixture by slow cooling. Compound **1f** was isolated as a yellow powder (2.00 g, 1.67 mmol) in 25% yield. ^1H NMR (CDCl_3 , 500 MHz): δ = 3.96 (s), 7.05 (d, J = 8.5 Hz), 7.34 (d, J = 8.5 Hz), 8.33 (d, J = 1.5 Hz), 8.61 (t, J = 1.5 Hz) ppm. ^{13}C NMR (CDCl_3 , 500 MHz): δ = 52.77 (CH_3), 88.35 ($\text{C}\equiv\text{C}$), 91.38 ($\text{C}\equiv\text{C}$), 121.41, 124.50, 130.29, 131.18, 131.67, 131.71, 136.68, 141.32, 143.59 (central $\text{C}=\text{C}$), 165.82 ($\text{C}=\text{O}$) ppm. IR (neat, cm^{-1}): 1729 (vs), 1596 (w), 1505 (w), 1439 (m), 1349 (m), 1244 (vs), 1195 (w), 1151 (m), 1106 (w), 1001 (m), 912 (w), 871 (w), 837 (w), 754 (s), 723 (w). MS (MALDI, m/z) 1196 (M^+ , 100%). Elemental analysis calculated for $\text{C}_{74}\text{H}_{52}\text{O}_{16}$: C, 74.23; H, 4.38. Found: C, 74.20; H, 4.34.

Tetrakis(1-(3,5-dicarboxy-phenyl-1-ethynyl)-4-phenyl)ethylene ($C_{66}H_{36}O_{16} \cdot 2H_2O$, $H_8TDPEPE$, **1g**). Methanol, THF, and distilled water were deoxygenated by sparging with nitrogen for at least 30 minutes. Compound **1f** (1.00 g, 0.835 mmol) was suspended in deoxygenated methanol (30 mL) and THF (20 mL). In a separate flask, sodium hydroxide (0.840 g, 0.021 mol) was dissolved in deoxygenated water (20 mL). The sodium hydroxide solution was added to the suspension of **1f** under nitrogen and the reaction mixture was heated to reflux for 24 hours. The mixture was cooled to room temperature and 50 mL of water was added. The solution was acidified with 60 mL of a 1M solution of aqueous HCl, causing the formation of a yellow precipitate. The yellow solid was washed with water and dichloromethane. The product was isolated as a yellow solid (0.739 g, 0.659 mmol) in 79% yield. 1H NMR (DMSO- d_6 , 500 MHz): δ = 7.07 (d, J = 8 Hz), 7.46 (d, J = 8 Hz), 8.22 (m), 8.43 (m), 13.52 (s) ppm (Figure S7). ^{13}C NMR (DMSO- d_6 , 500 MHz): δ = 88.14 (C \equiv C), 90.83 (C \equiv C), 120.39, 123.33, 129.76, 131.27, 131.47, 132.05, 135.57, 140.81, 143.21 (central C=C), 165.85 (C=O) ppm (Figure S8). IR (neat, cm^{-1}): 3087 (m, br), 1704 (vs), 1597 (m), 1504 (w), 1444 (m), 1405 (m), 1268 (s), 1242 (s), 1164 (m), 1110 (w), 914 (w), 836 (w), 811 (w), 758 (m), 671 (m). MS (MALDI, m/z) 1084 (M^+ , 100%). Elemental analysis calculated for $C_{66}H_{36}O_{16} \cdot 2H_2O$: C, 70.71; H, 3.60. Found: C, 70.46; H, 3.60.

[Zn₄(TDPEPE)(H₂O)₄(DEF)₄]·(H₂O)₃(DEF)_{9.5} ($Zn_4C_{133.5}H_{190.5}N_{13.5}O_{36.5}$, **1**). Solutions of $Zn(NO_3)_2 \cdot 6H_2O$ (150 mg, 0.504 mmol) in 3 mL of ethanol and $H_8TDPEPE$ (12.8 mg, 0.011 mmol) in 3 mL of DEF were mixed, filtered, and placed in a 20 mL scintillation vial. The vial was capped and heated inside an isothermal oven at 75 °C for 36 h. Yellow crystalline blocks of **1** (25.0 mg, 8.83 μ mol) were isolated in 77% yield. IR (neat, cm^{-1}): 2978 (w), 2940 (w), 2883 (w), 1638 (vs), 1583 (m), 1430 (s), 1373 (s), 1307 (w), 1266 (w), 1215 (w), 1106 (w), 777 (w), 722 (w). Elemental analysis calculated for $Zn_4C_{133.5}H_{190.5}N_{13.5}O_{36.5}$: C, 56.34; H, 6.48; N, 7.00. Found: C, 56.66; H, 6.78; N, 6.68.

Computational Details. Calculations were performed using the ORCA 2.9 quantum chemistry program package from the development team at the Max Planck Institute for Bioinorganic Chemistry.⁵ In all cases the LDA and GGA functionals employed were those of Perdew and Wang (PW-LDA, PW91).⁶ Calculations were performed using the TZV basis set

for hydrogen and the TZV(p) basis set for the main group atoms.⁷ Spin-restricted Kohn–Sham determinants were chosen to describe the closed-shell wavefunctions, employing the RI approximation and the tight SCF convergence criteria provided by ORCA. Constrained potential energy surfaces were constructed by fixing the Cartesian coordinates of the carboxylic oxygen atoms and varying one C_{Ar}–C_{Ar}–C=C dihedral angle while the remaining coordinates were allowed to relax. Ligand strain energies were determined by replacing the metal nodes with hydrogen atoms and taking the difference in energy between the ligand with the framework geometry preserved (allowing only the hydrogen atom positions to optimize) and the ligand with the geometry relaxed under no constraints.

X-ray crystal structure determination. A diffraction-quality single crystal of **1** was mounted on a MiTeGen MicroMount (Ithaca, NY) using Paratone-N oil. Low temperature (100 K) diffraction data (ϕ - and ω -scans) were collected on a Bruker-AXS X8 Kappa Duo diffractometer coupled to a Smart APEX II CCD detector with MoK α radiation ($\lambda = 0.71073 \text{ \AA}$) from a $I\mu S$ microfocus source. Absorption and other corrections were applied using SADABS.⁸ The structure was solved by direct methods using SHELXS⁹ and refined against F^2 on all data by full-matrix least squares as implemented in SHELXL-97.⁹ Due to the large amount of spatially delocalized electron density in the pores of the lattice, acceptable refinement values could not be obtained for this electron density. Instead, the best residual indices were obtained from a model for which the program SQUEEZE¹⁰ was used to account for the electron density in regions of high solvent disorder. All non-hydrogen atoms of the framework were refined anisotropically. Hydrogen atoms pertaining to the ligand were included in the model at geometrically calculated positions using a riding model. The crystallographic data for **1** are shown in Table S2.

Fluorescence and UV-Vis Spectroscopy. Steady-state emission spectra were acquired on a Horiba Jobin-Yvon SPEX Fluorolog-3 (model FL3-21, 450 W Xenon lamp) with excitation and emission slit widths of 3 and 5 nm, respectively. Emission measurements on solid samples were collected in front-face mode on the single crystals of the appropriate materials placed on the glass microscope slides. Diffuse reflectance spectra were collected on a Varian

Cary 5000 UV-vis-NIR spectrometer equipped with a Praying Mantis diffuse reflectance accessory (Harrick Scientific Products) and referenced to barium sulfate.

Other physical measurements.

Infrared spectra were obtained on a Bruker TENSOR 37 FT-IR Spectrometer equipped with a Pike Technologies GladiATR attenuated total reflectance accessory. Solution NMR spectra were collected on a Varian 300 or a Varian Inova-500 NMR spectrometer. ^{13}C and ^1H spectra were referenced to natural abundance ^{13}C peaks and residual ^1H peaks of deuterated solvents, respectively. Powder X-ray diffraction patterns were recorded on a Bruker Advance D8 diffractometer using Nickel-filtered Cu-K α radiation ($\lambda = 1.5418 \text{ \AA}$), with accelerating voltage and current of 40 kV and 40 mA, respectively.

References:

1. Z. Li, M. Siklos, N. Pucher, K. Cicha, A. Ajami, W. Husinsky, A. Rosspeinter, E. Vauthey, G. Gescheidt, J. Stampfl, R. Liska, *J. Polym. Sci., Part A: Polym. Chem.*, **2011**, *49*, 3688–3699.
2. E. W. Kwock, Jr. T. Baird, T. M. Miller *Macromol.*, **1993**, *26*, 2935–2940.
3. K. Tanaka, T. Hiratsuka, Y. Kojimab, Y. T. Osano, *J. Chem. Research (S)*, **2002**, 2009–2012.
4. T. Shiraishi, Y. Kitamura, Y. Ueno, Y. Kitade, *Y. Chem. Commun.*, **2011**, *47*, 2691–2693.
5. F. Neese *ORCA—an ab initio, Density Functional and Semiempirical program package, version 2.9.0, 2012*.
6. J. P. Perdew, Y. Wang, *Phys. Rev. B*, **1992**, *46*, 12947–12954.
7. A. Schafer, H. Horn, R. Ahlrichs *J. Chem. Phys.*, **1992**, *97*, 2571–2577.
8. G. M. Sheldrick *SADABS - A program for area detector absorption corrections 2004*.
9. G. M. Sheldrick *Acta Cryst. Sect. A*, **1990**, *46*, 467–473.
10. T. Spek SQUEEZE, 1999.

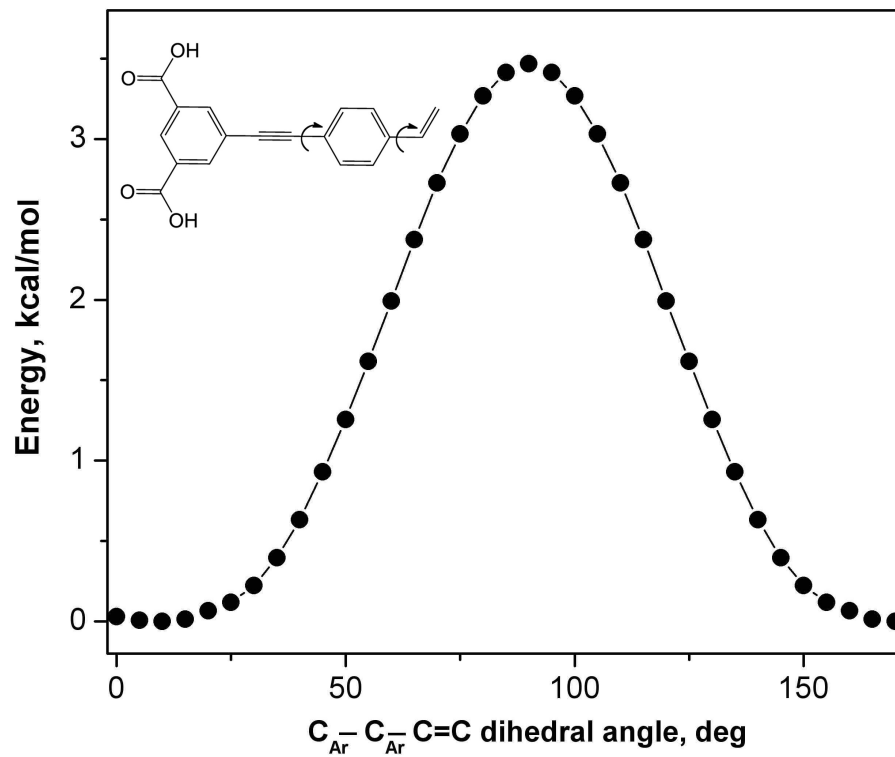


Figure S1. DFT-calculated potential energy surface for phenyl ring flipping in 5-((4-vinylphenyl)ethynyl)isophthalic acid. Lines have been added as a visual guide.

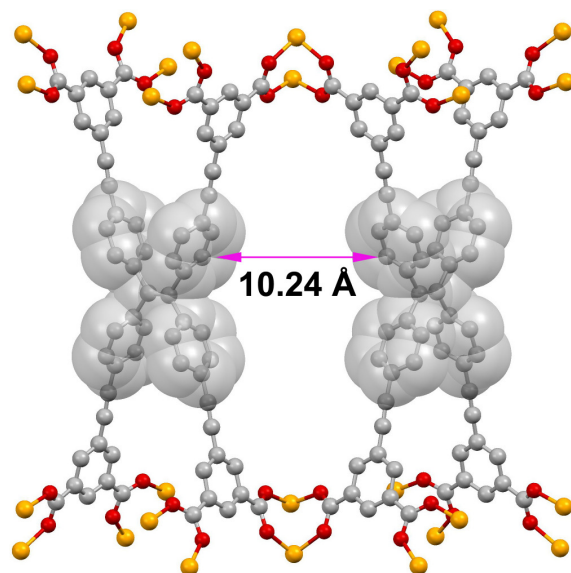


Figure S2. The shortest chromophore-chromophore contacts (phenyl ring centroid-centroid distances) in **1**.

Table S1. X-ray structure refinement data^a for **1**.

formula	Zn ₄ (C ₆₆ H ₂₈ O ₁₆)
FW	1338.48
<i>T</i> , K	100(1)
crystal system, space group	Tetragonal, I4/mmm
<i>Z</i>	8
<i>a</i> , Å	18.765(3)
<i>b</i> , Å	18.765(3)
<i>c</i> , Å	46.463(12)
<i>V</i> , Å ³	16361(7)
<i>d</i> _{calc} , g/cm ³	0.569
μ , mm ⁻¹	0.608
<i>F</i> (000)	2816.0
crystal size, mm	0.03×0.05×0.05
theta range	1.99 to 26.35
index ranges	-20 ≤ <i>h</i> ≤ 20 -18 ≤ <i>k</i> ≤ 20 -50 ≤ <i>l</i> ≤ 51
refl. collected	44546
data/restraints/parameters	3364 / 111 / 116
GOF on <i>F</i> ²	0.885
large peak/hole, e/Å ³	0.135/-0.135
<i>R</i> ₁ (<i>wR</i> ₂), %, [<i>I</i> >2σ(<i>I</i>)] ^b	5.42(15.73)

^a Mo-Kα ($\lambda = 0.71073$ Å) radiation^b $R_1 = \sum ||F_o| - |F_c|| / \sum |F_o|$, $wR_2 = \{ \sum [w(F_o^2 - F_c^2)^2] / \sum [w(F_o^2)^2] \}^{1/2}$

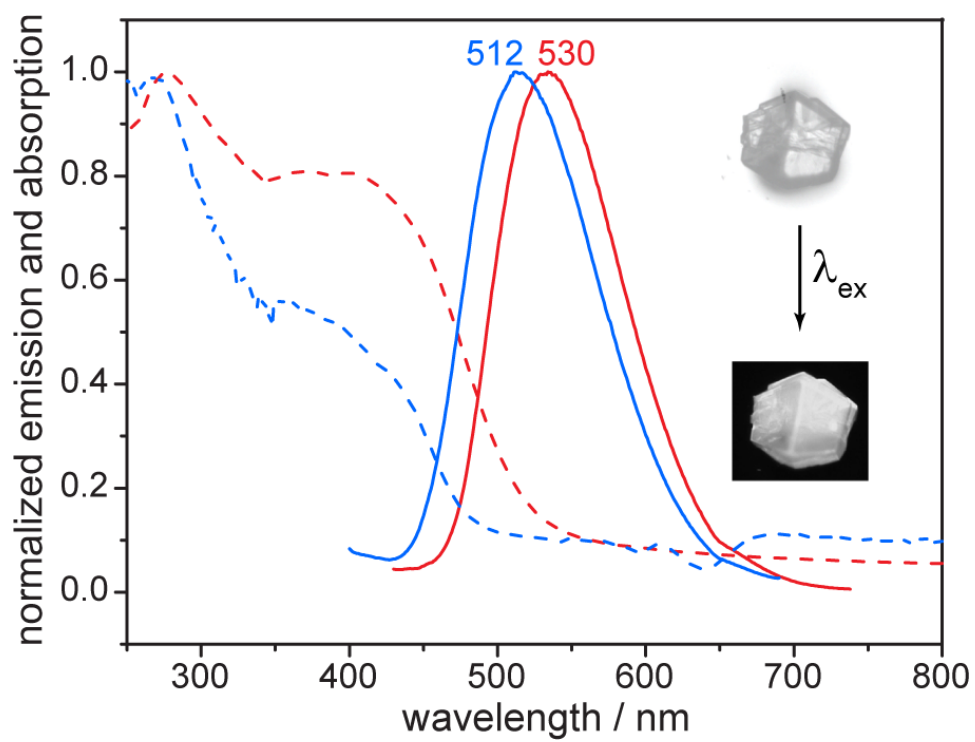


Figure S3. Normalized absorption (- - -) and emission (—) spectra for **1** (purple) and H₈TDPEPE (red). The inset shows an epifluorescence micrograph of a crystal of **1** before and after irradiation.

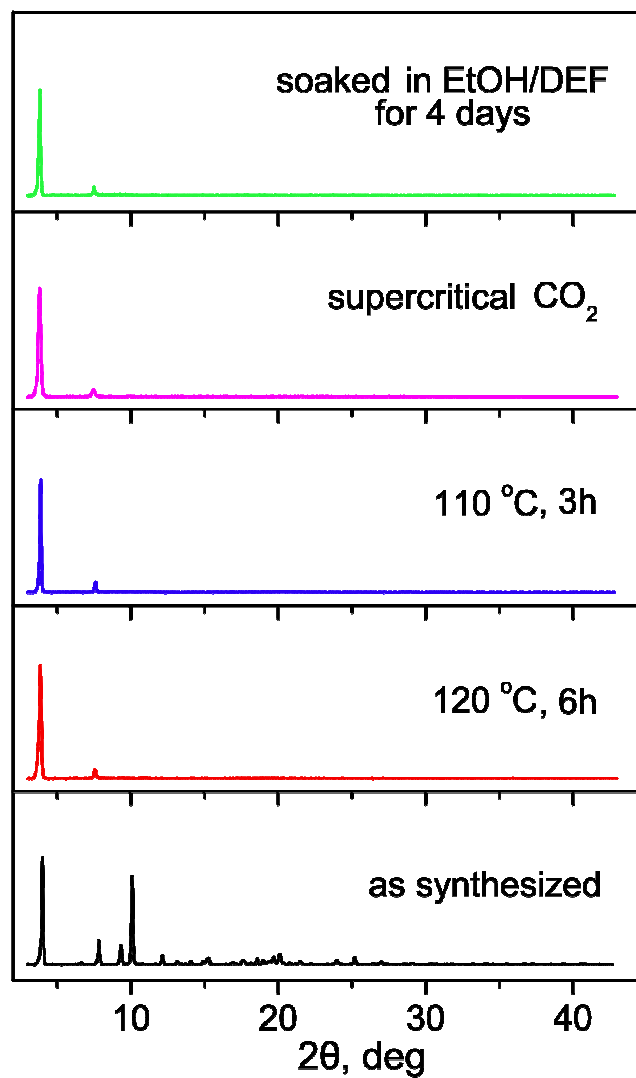


Figure S4. PXRD patterns of **1**: as synthesized (black), heated at 120 °C for 6 h (red), heated at 110 °C for 3 h (blue), treated using a supercritical CO_2 technique (purple), and soaked in EtOH/DEF solution for 4 days.

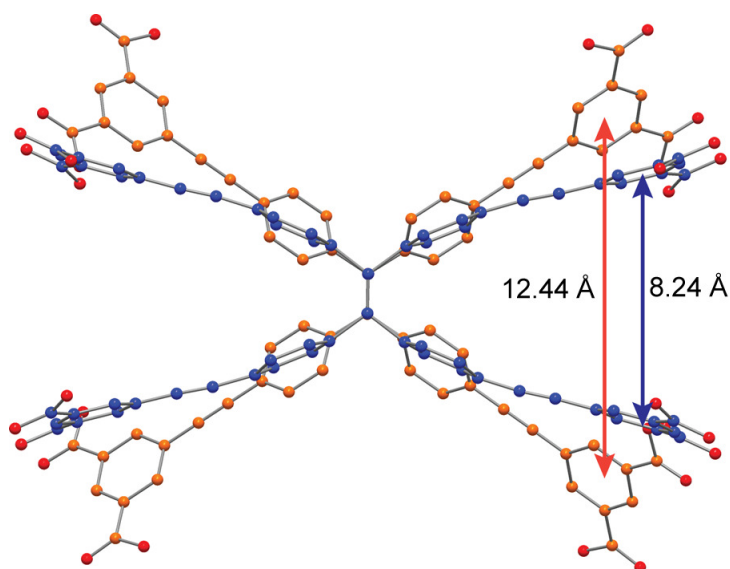


Figure S5. Overlay of the conformations of H₈TDPEPE as predicted by DFT (orange C atoms), and H₈TDPEPE⊂1* (blue C atoms). The centroid-centroid distances between the isophthalate units are used to illustrate the strain imposed onto TDPEPE⁸⁻ by coordination within **1**. Red spheres represent O atoms. H atoms were removed for clarity.

* Here H₈TDPEPE⊂1 denotes the protonated ligand that is locked in the conformation of the ligand as it is found in the framework. The same formalism is used in Figures S9–S17.

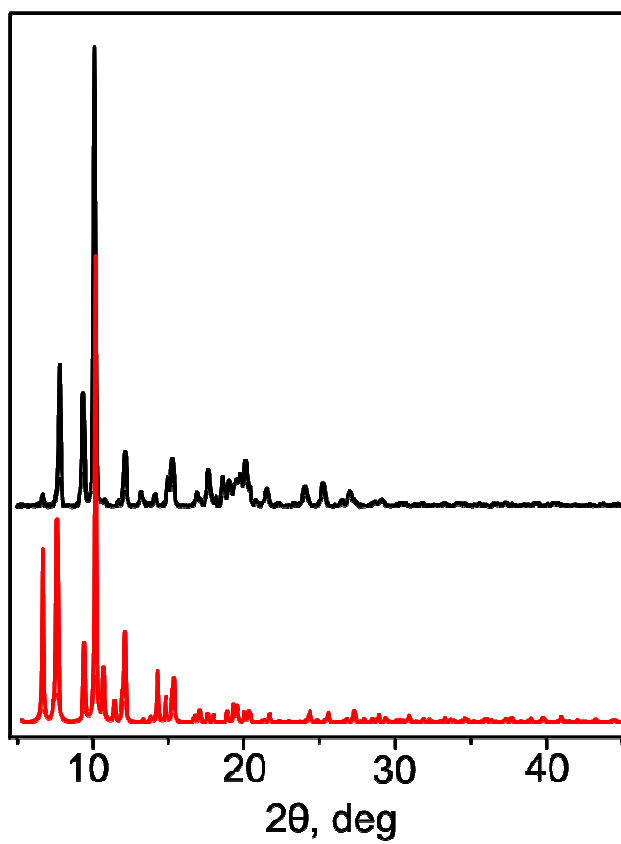


Figure S6. Simulated (red) and experimental (black) PXRD patterns of **1**.

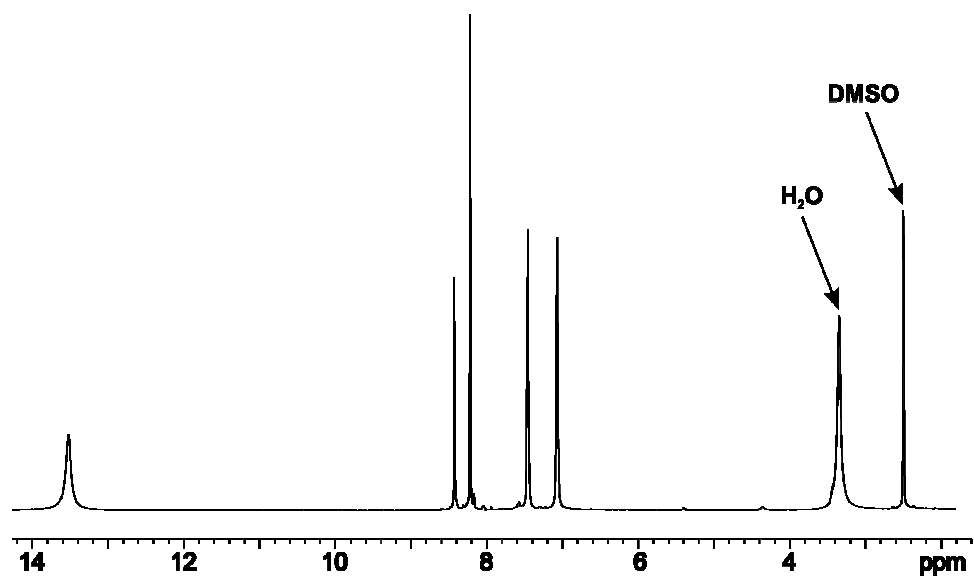


Figure S7. ^1H NMR spectrum of H_8TDPEPE in $\text{DMSO-}d_6$ (500 MHz).

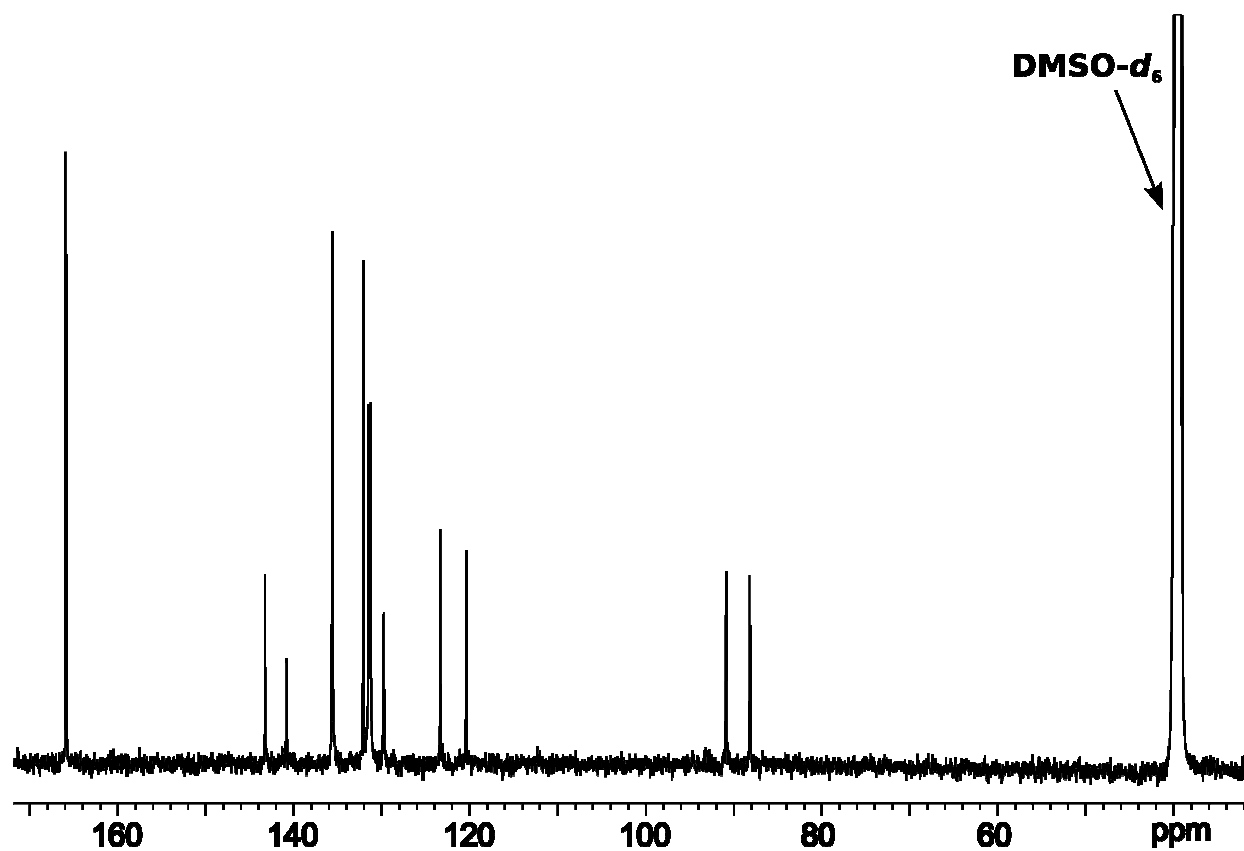


Figure S8. ^{13}C NMR spectrum of H_8TDPEPE in $\text{DMSO-}d_6$ (500 MHz).

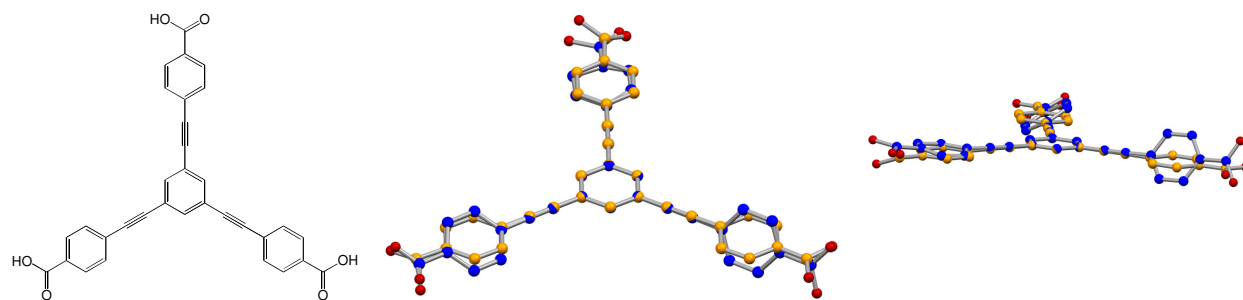


Figure S9. (left) Ligand H₃BTE. (middle, right) Overlays of the conformations of H₃BTE as predicted by DFT (orange C atoms), and of H₃BTE@MOF-180 (blue C atoms). Red spheres represent O atoms. H atoms were removed for clarity.

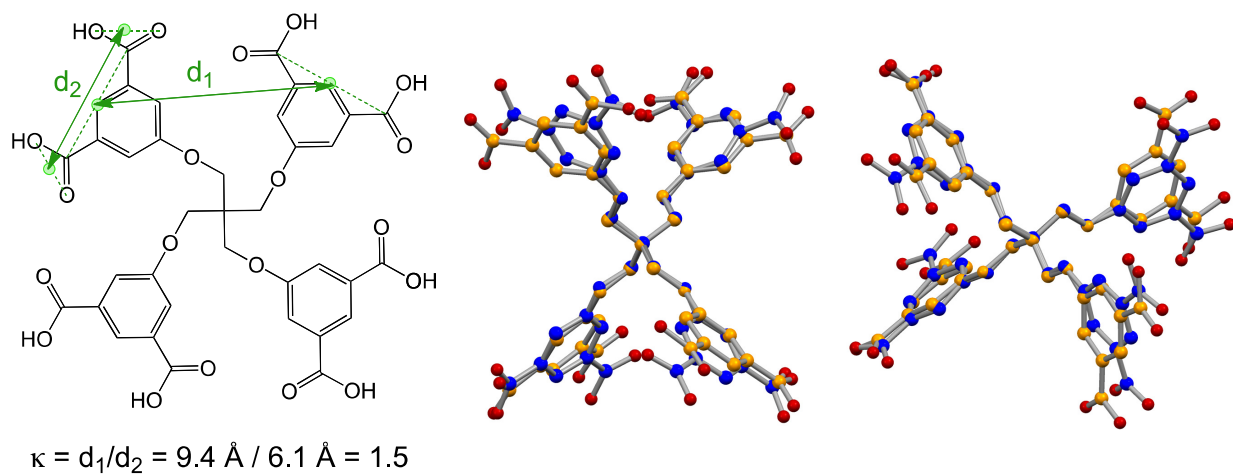


Figure S10. (left) Ligand H₈TDM. Filled green circles represent centroids of two carbon atoms in carboxylic groups and centroids of two oxygen atoms. (middle, right) Overlay of the conformations of H₈TDM as predicted by DFT (orange C atoms), and of H₈TDM@PCN-26 (blue C atoms). Red spheres represent O atoms. H atoms were removed for clarity.

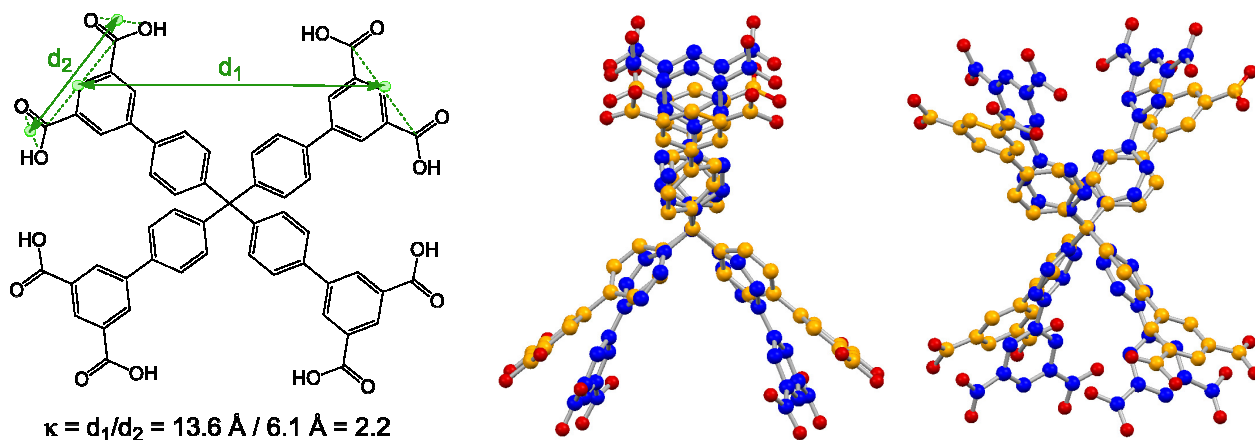


Figure S11. (left) Ligand H₈MTBD. Filled green circles represent centroids of two carbon atoms in carboxylic groups and centroids of two oxygen atoms. (middle, right) Overlay of the two conformations of H₈MTBD as predicted by DFT (orange C atoms), and as observed in H₈MTBD@NOCTT-140 (blue C atoms). Red spheres represent O atoms. H atoms were removed for clarity.

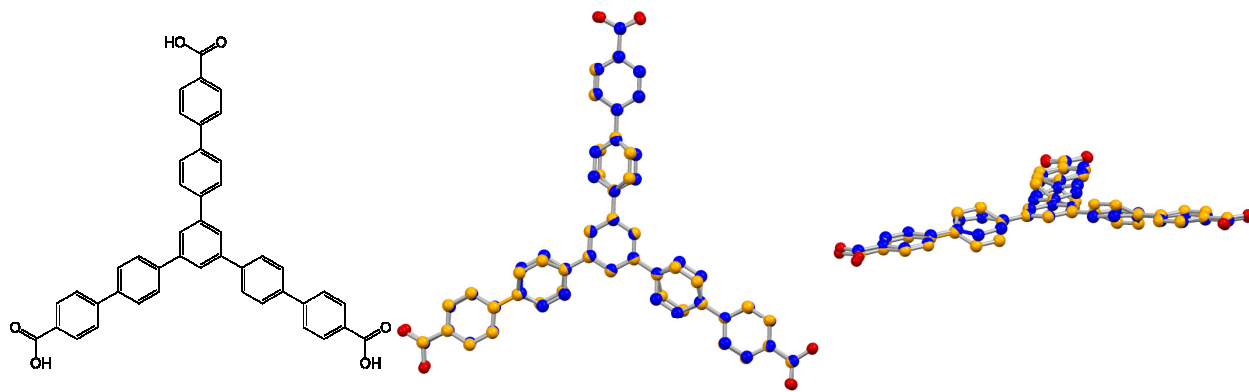


Figure S12. (left) Ligand H₃BBC. (middle, right) Overlay of the conformations of H₃BBC as predicted by DFT (orange C atoms), and of H₃BBC@MOF-200 (blue C atoms). Red spheres represent O atoms. H atoms were removed for clarity.

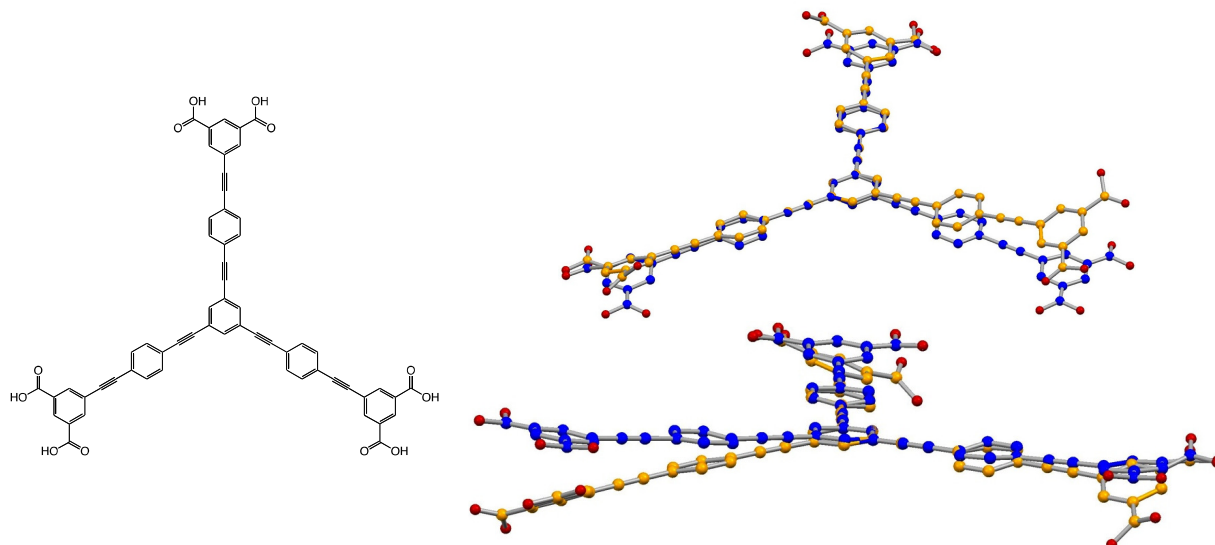


Figure S13. (left) Ligand H₆TCAEPEB. (right) Overlay of the conformations of H₆TCAEPEB as predicted by DFT (orange C atoms), and of H₆TCAEPEB-NU-100 (blue C atoms). Red spheres represent O atoms. H atoms were removed for clarity.

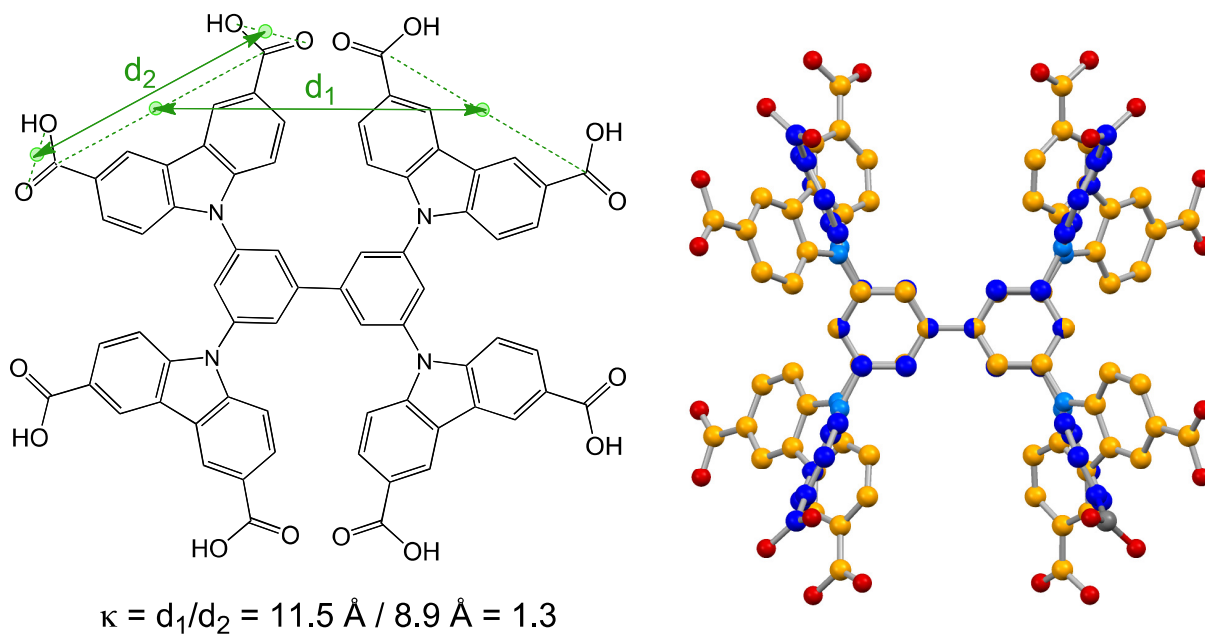
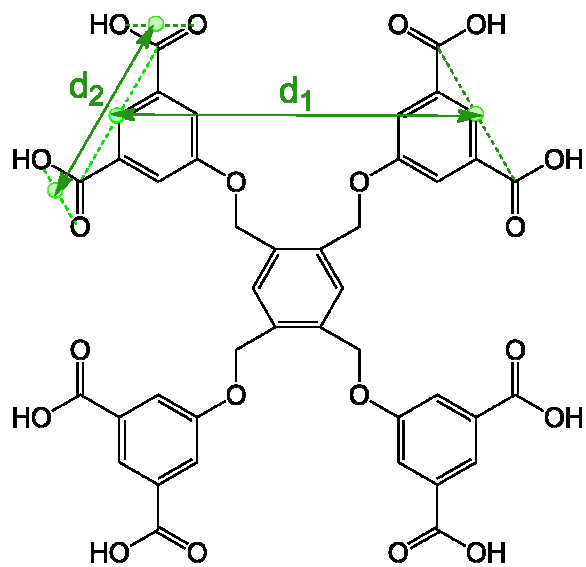


Figure S14. (left) Ligand H₈BTTCD. Filled green circles represent centroids of two carbon atoms in carboxylic groups and centroids of two oxygen atoms. (right) Overlay of the conformations of H₈BTTCD as predicted by DFT (orange C atoms), and of H₈BTTCD⊂PCN-80 (dark blue C atoms). Red and light blue spheres represent O and N atoms, respectively. H atoms were removed for clarity.



$$\kappa = d_1/d_2 = 7.44 \text{ \AA} / 6.08 \text{ \AA} = 1.2$$

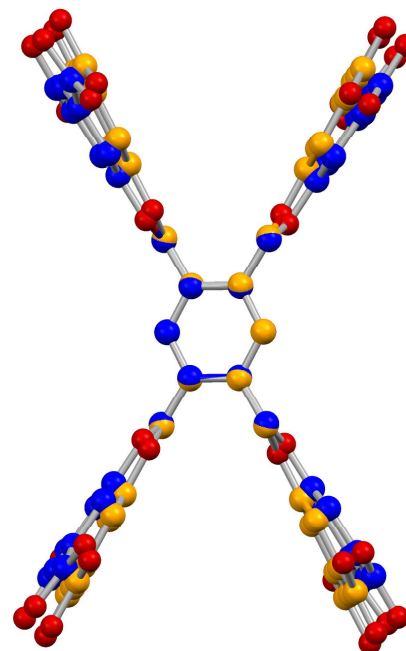


Figure S15. (left) Ligand H₈PTMT. Filled green circles represent centroids of two carbon atoms in carboxylic groups and centroids of two oxygen atoms. (right) Filled green circles represent centroids of two carbon atoms in carboxylic groups and centroids of two oxygen atoms. Overlay of the conformations of H₈PTMT as predicted by DFT (orange C atoms), and of H₈PTMT-Cu₄(PTMT)(H₂O)₄ (blue C atoms). Red spheres represent O atoms. H atoms were removed for clarity.

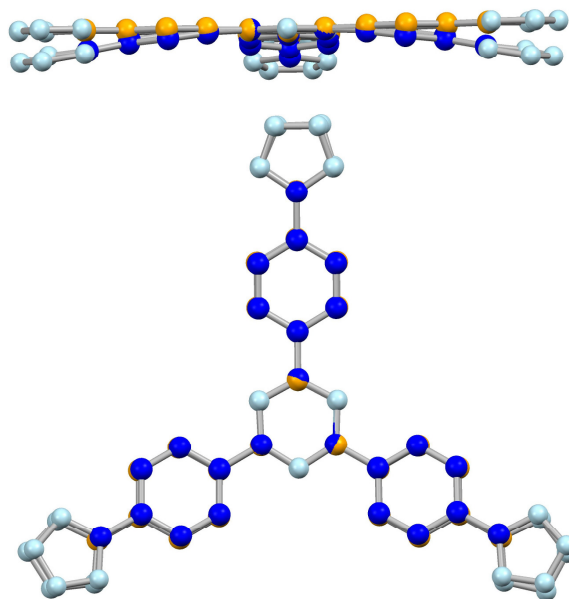
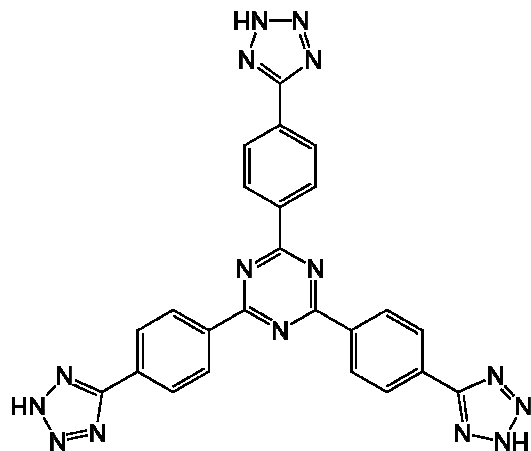


Figure S16. (left) Ligand H₃TPT-3tz. (right) Overlay of the conformations of H₃TPT-3tz as predicted by DFT (orange C atoms), and of H₃TPT-3tzMn₃[(Mn₄Cl)₃(TPT-3tz)₈]₂ (dark blue C atoms). Light blue spheres represent N atoms. H atoms were removed for clarity.

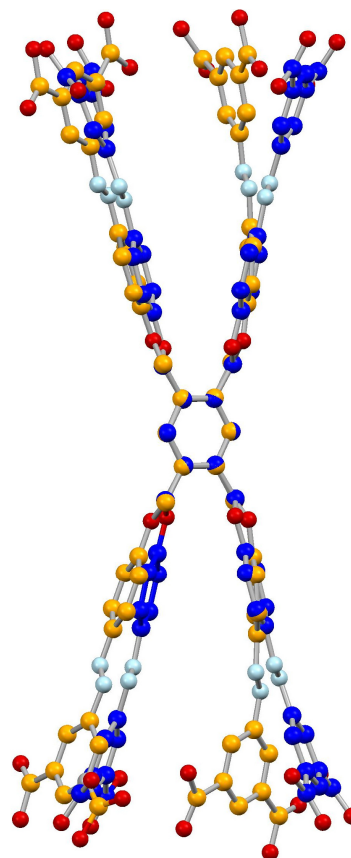
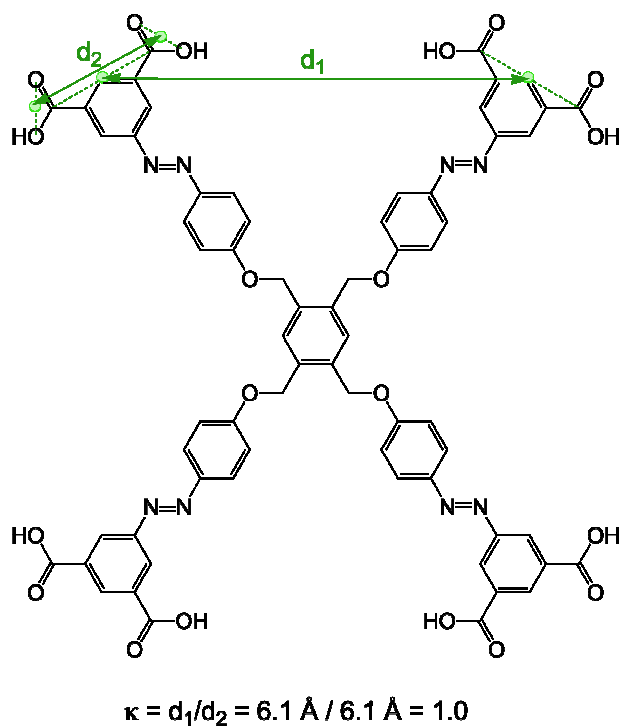


Figure S17. (left) Ligand H₈BTMPT. Filled green circles represent centroids of two carbon atoms in carboxylic groups and centroids of two oxygen atoms. (right) Overlay of two conformations of H₈BTMPT as predicted by DFT (orange C atoms), and as observed in H₈BTMPT·Cu₄(BTMPT)(H₂O)₄ (dark blue C atoms). Light blue and red spheres represent N and O atoms, respectively. H atoms were removed for clarity.

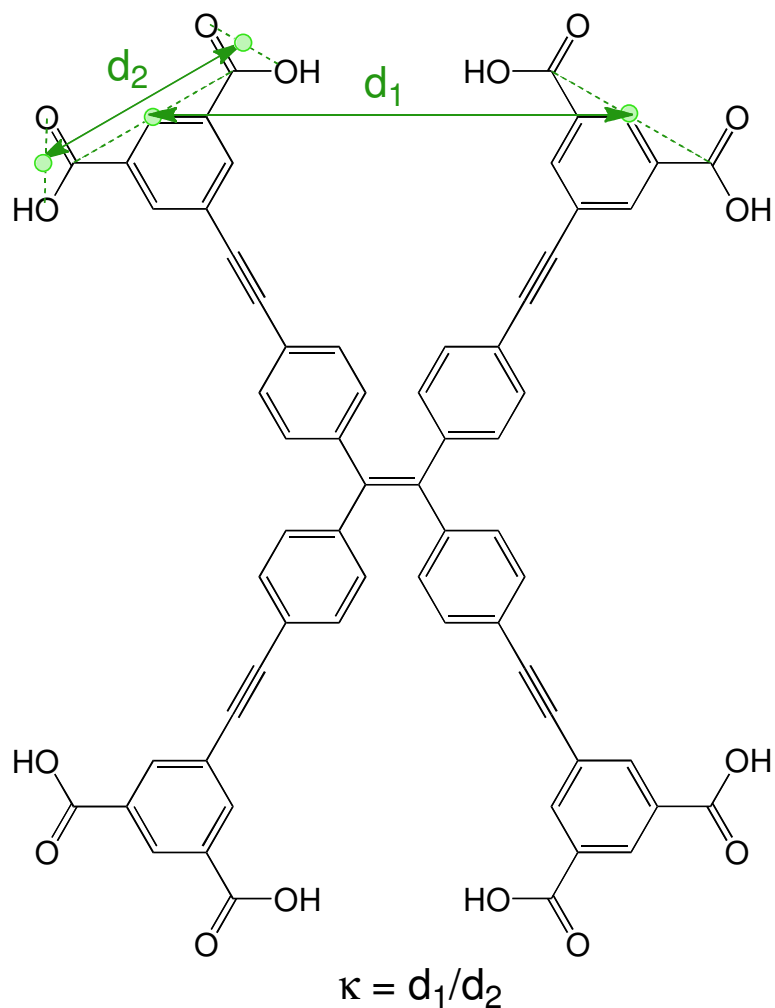


Figure S18. Definition of d_1 and d_2 : to determine d_1 , centroids are first formed between the C atoms of carboxylate groups on the same arm (here, centroids are formed between the C atoms of the carboxylic acid groups on isophthalate units). Second, these centroids are united between two arms, defining distance d_1 . Distance d_2 is the distance between centroids defined by O atoms on carboxylate groups on the same arm (for $H_8TDPEPE$, the isophthalate groups). See Figure S14 for an example that does not contain isophthalate groups.